



University of Glasgow
DEPARTMENT OF

**AEROSPACE
ENGINEERING**



Mathematical Definition of Helicopter Manoeuvres

Dr Douglas G. Thomson*

Roy Bradley†

Internal Report No. 9225

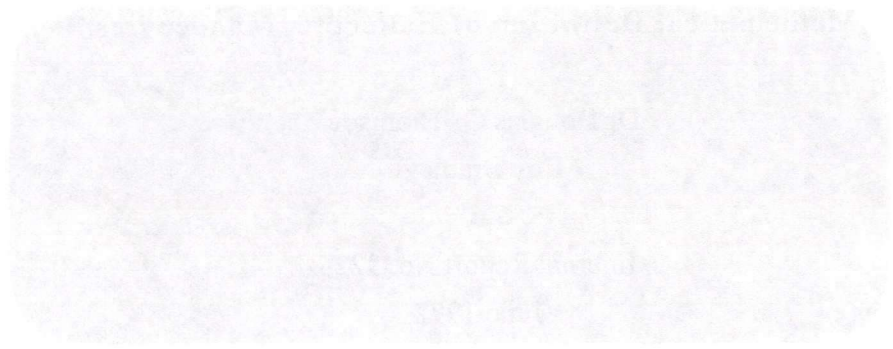
June 1992

Engineering
PERIODICALS

U7000



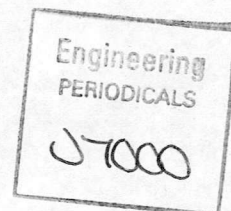
10
1000



Senior Lecturer
Royal Society University Research Fellow

Department of Aerospace Engineering
University of Glasgow
Glasgow
G12 8QQ





Mathematical Definition of Helicopter Manoeuvres

Dr Douglas G. Thomson*

Roy Bradley†

Internal Report No. 9225

June 1992

*Royal Society University Research Fellow

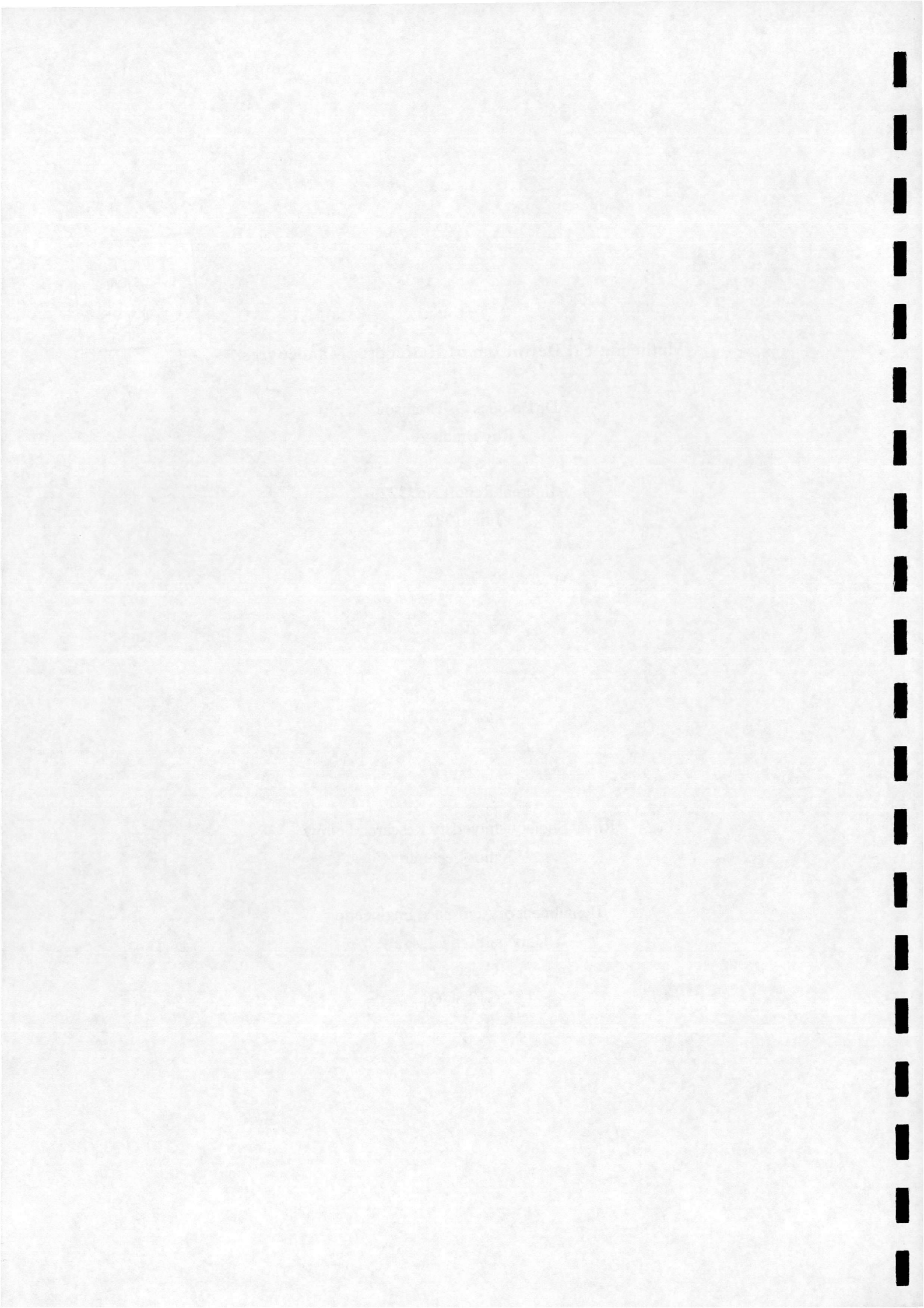
†Senior Lecturer

Department of Aerospace Engineering

University of Glasgow

Glasgow

G12 8QQ



Abstract

There is an increasing number of flight mechanics studies where the influence of manoeuvre type has been found to be of importance. A notable example has been the upgrade to the U.S. Mil. Spec. for handling qualities which includes a set of aggressive tasks to be flown as part of the flight test requirements. Another recent development has been the wider use of inverse simulation where a flight path is used to drive a helicopter mathematical model, the aim being to calculate the control actions corresponding to the flight path being flown. Although the evaluation of helicopter performance through the use of standard manoeuvres has become established, there is little information available on the precise form of the manoeuvre, or on how mathematical representations may be constructed. The aim of this paper has been to categorise the various types of manoeuvre commonly used in helicopter military operations, and then to develop algorithms capable of defining them mathematically. Several manoeuvres are fully modelled in the paper, and it becomes apparent that the techniques used may be applied to a variety of different manoeuvres. By way of validation, data from flight tests has been used for comparisons with modelled flight paths and manoeuvre parameters. Methods of grading manoeuvres are also presented along with a discussion on the choice of suitable mathematical functions.

Nomenclature

| | | | |
|----------------|---|--------------------------------|--|
| C_T | Thrust coefficient | T | Main rotor thrust (N) |
| C_w | Weight coefficient | t_m | Manoeuvre time (s) |
| g | Acceleration due to gravity (m/s^2) | V | Flight velocity (m/s) |
| h | Height above xy plane (m) | V_{max} | Maximum velocity attained (m/s) |
| k | Fraction of turn manoeuvre spent in entry and exit transients | \dot{V} | Acceleration along flight path (m/s^2) |
| m | Mass of helicopter (kg) | $\dot{x}, \dot{y}, \dot{z}$ | Component velocitiesd (m/s) |
| n_{fp} | Flight path load factor | $\ddot{x}, \ddot{y}, \ddot{z}$ | Component accelerations (m/s) |
| n_p | Load factor normal to flight path | x_e, y_e | Flight path coordinates at turn exit (m) |
| n_t | Load factor tangential to flight path | χ | Track angle (rad) |
| n_{Th} | Thrust factor | $\dot{\chi}$ | Turn rate (rad/s) |
| n_{θ_0} | Collective factor | χ_e | Track angle at exit from turn (rad) |
| R | Rotor radius (m) | $\dot{\chi}_m$ | Maximum turn rate (rad/s) |
| R_c | Radius of circular track (m) | γ | Angle of climb (rad) |
| R_e | Equivalent circular track radius (m) | θ_0 | Main rotor collective pitch angle (rad) |
| s | Distance around track (m) | ρ | Density of air (kg/m^3) |
| t | Time (s) | Ω | Rotational speed of main rotor (rad/s) |

1. Applications and Origins of Standard Manoeuvres for Helicopters

A significant element in the assessment of all aircraft is their performance in the execution of a variety of standard manoeuvres. For fixed wing aircraft the manoeuvres may include take-off, landing, turning and vertical loop, while for rotorcraft their versatility has led to their use in a variety of applications each of which may possess its own characteristic type of manoeuvre. Take-off and landing are, of course, universal manoeuvres for rotorcraft, Figure 1, for example, shows the take off requirements as specified by the Federal Aviation Authority, [1, 2]. Before a helicopter is certified airworthy, the manufacturer must show that the requirements specified by certifying body (the FAA in the United States, for example) can be met. In the case of the take-off manoeuvre shown in Figure 1, the manufacturer must determine the normal take-off distance in a range of atmospheric conditions (temperature and altitude) and configurational conditions (centre of gravity position, one engine inoperative etc.) given that a height of 50ft. must be reached. To some extent, therefore, the certifying body has defined the shape of the manoeuvre. In the landing case, a certain amount of forward speed is desirable to avoid the vortex ring condition, while, in the take-off, safety considerations may require a certain angle of climb in order to maximise the chance of survival in the event of engine failure. This condition is shown in Figure 1 where safety regulations require the manufacturer to show that the helicopter can perform a safe landing should there be an engine failure at the Critical Decision Point (CDP) during take-off.

In the military sphere of operation there has been considerable development of strategies and techniques for the use of attack helicopters in battlefield situations, including nap-of-the-earth (NOE) operations, where many standard manoeuvres have been devised and employed. The manoeuvres can be conveniently grouped into four headings :- obstacle avoidance, concealment, weapons aiming and delivery, and target acquisition and tracking. As examples of these we have, in Figure 2, the hurdle-hop manoeuvre, used to avoid an obstacle of a certain height by overflying it then returning to the initial lower altitude for concealment. Figure 3 illustrates a Side-step which is a repositioning manoeuvre between areas of cover, and Figure 4 shows the Bob-up which is a vertical repositioning manoeuvre which is used for weapons delivery especially when the helicopter is equipped with a mast mounted sight. Finally, Figure 5 shows a ground target acquisition manoeuvre known as the Tear-drop Turn. The precision with which these manoeuvres are defined varies between applications. The recently published handling qualities specification [3] contains several manoeuvres, defined in terms of the required flight path, which must be achievable with Level 1 handling (minimal, or no, pilot compensation required for desired performance, [3]). The basic manoeuvres of the handling qualities document are Mission Task Elements (MTE's) and, as their name suggests, they are considered to be the building blocks of an operational mission as far as handling qualities are

concerned - representing those parts of the mission where the quality of the helicopter handling is a key parameter. The Bob-up and Side-step are incorporated in the list of MTE's along with several others including the Quick-Hop, Figure 6, (referred to as "Rapid Acceleration and Deceleration").

It is apparent that both the authors of the FAA regulations, and the Mil. Spec. Requirements have gone some way towards producing precise definitions of manoeuvres. In particular, several of the MTE's in Reference 3 are described in terms of flight path, attitude and velocity limits. Although the descriptions do leave some scope for interpretation, in general, the tasks involved are clear to the pilot, so that they are more than adequate for handling qualities flight test purposes. However there are several reasons for seeking to develop techniques for providing a more complete, mathematical description of standard classes of manoeuvre. First, it is likely that the trend to a more closely defined set of requirements will continue and it is necessary to develop an appropriate vocabulary in which to express them. Second, any attempt at classification of manoeuvres, such as grading their severity, will need a standardised description, and third, any assessment of compliance with requirements by simulation requires a mathematical formulation of the manoeuvre. In this context it is inverse simulation (defined as the computation of the control inputs to a dynamic system necessary to produce a desired output state) that is most relevant. In the case of helicopter flight, the output state can be expressed in terms of a flight path, and the calculated inputs are, of course, the pilot's control displacements : main rotor collective, longitudinal and lateral cyclic, and tail rotor collective. A computer package capable of performing inverse simulations for helicopters, HELINV, has been developed at the University of Glasgow [4], and has been used for several flight mechanics studies [5, 6, 7]. One of the most recent applications [8] has been a study which has confirmed the validity of the inverse simulation algorithm, and also contributed towards the validation of the mathematical model used - the Royal Aerospace Establishment's (RAE) HELISTAB model [9]. A complete discussion of the inverse simulation algorithm can be found in References 4 and 5. As a result of this work a substantial body of experience has been gained in the mathematical representation of helicopter manoeuvres, and the options available for describing them. This paper describes the techniques which have been developed and gives examples of the main types. Some of the flight paths can be described in terms of explicit expressions, but in many cases a sequence of calculations is involved which may include an iterative element. For this reason the formal manoeuvre descriptions are referred to as manoeuvre defining algorithms. The authors are not aware that this material is available elsewhere in the aeronautical literature.

Examples of specific manoeuvres are given in Section 3 after the manoeuvre defining algorithms have been introduced in Section 2. Validation of the flight path definitions is

discussed in Section 4, and some comparisons with flight data are made. The following sections, 5 and 6, consider the questions of grading the severity of manoeuvres and the order of representation respectively. Finally, in Section 7, some conclusions are expressed about the progress made so far, and the issues remaining.

2. Requirements for Manoeuvre Defining Algorithms

It is convenient to discuss the requirements for the definition of manoeuvres initially in relation to the needs of the HELINV package, since these are quite explicit. Subsequently their more general applicability will become clear. The basis of HELINV is the ability to calculate the control displacements required to produce a predefined unsteady flight condition. It is necessary that before the control angles are calculated, the rotor thrust, and its direction, must be found. This will require knowledge of the velocity and acceleration of the helicopter, from which the force and moment components (inertial, gravitational and aerodynamic) may be estimated. The first, and most basic requirement of the manoeuvre-defining algorithm is therefore that it must be able to compute the velocities and accelerations of the helicopter throughout the manoeuvre. As the simulation is in the form of a time response, it follows that the velocities and accelerations will be expressed as functions of time.

The only other major requirement of the manoeuvre-modelling algorithms is that the analytical functions defining flight path definitions must display a physically realistic degree of continuity. In the case of a helicopter inverse simulation, the flight path acts as the input to the system. It follows that if the input is discontinuous then it will act on the system in a way similar to a series of step inputs, and it has been shown [10] that the effect on the vehicle response can be unrepresentative. Lack of appropriate smoothness in the flight path can occur, in particular, where curved and linear sections are joined or, in general, at the joins of any piecewise representation.

It is often convenient in flight-mechanics modelling to set up earth fixed and body fixed origins and frames of reference. This allows the flight condition of the aircraft to be expressed in the earth axes frame, hence, independently from the dynamics of the vehicle. The velocities and accelerations expressed in earth axes can be transformed through the Euler angles, Figure 7, to give their body fixed equivalents, and vice versa. Conventionally, the earth origin is located arbitrarily with the earth x-axis pointing northward, the y-axis eastward, and the z-axis pointing vertically downwards. In this paper, for convenience, the origin is positioned at the entry to the manoeuvre, and it is assumed that at the entry point, the helicopter's flight velocity vector is pointing in the earth x-axis direction. The position of the helicopter is taken to be the

location, in the earth fixed frame, of the helicopter's centre of gravity. This is also normal practice as the body fixed origin is located at this point. To create a mathematical representation of a specific manoeuvre, the problem is then to express trajectory of the helicopter's centre of gravity position (x, y, z) within the earth axes system. If the flight velocity profile of the helicopter is also specified (preferably as a function of time) then it is possible to determine the components of earth axis velocities and accelerations (as functions of time) through the whole manoeuvre. This is necessary as the earth axes velocities and accelerations may then be transformed to the body fixed frame, hence allowing the aerodynamic and inertial forces and moments of the vehicle to be calculated.

2.1 A General Flight Path Definition

Before modelling specific manoeuvres, it will be useful to introduce the basic theory by describing a general three dimensional manoeuvre such as the climbing turn shown in Figure 8(a). Figure 8(b) shows the manoeuvre track which is taken to be the projection of the flight path in the xy plane, and Figure 8(c) shows the altitude change around the manoeuvre. The angle between the velocity vector and the x direction in the x-y plane is known as the track angle, χ , and the angle between the s-axis and the velocity vector in the x-s plane is the angle of climb, γ . From Figure 8 it is apparent that the components of velocity in the earth fixed axes can be related to the flight velocity, V, and flight path angles χ , γ , by the expressions

$$\dot{x} = V \cos\gamma \cos\chi \quad (1)$$

$$\dot{y} = V \cos\gamma \sin\chi \quad (2)$$

$$\dot{z} = -V \sin\gamma \quad (3)$$

The component accelerations of the helicopter are then found by differentiation to be

$$\ddot{x} = \dot{V} \cos\gamma \cos\chi - V\dot{\gamma} \sin\gamma \cos\chi - V \dot{\chi} \cos\gamma \sin\chi \quad (4)$$

$$\ddot{y} = \dot{V} \cos\gamma \sin\chi - V\dot{\gamma} \sin\gamma \sin\chi + V \dot{\chi} \cos\gamma \cos\chi \quad (5)$$

$$\ddot{z} = -\dot{V} \sin\gamma - V\dot{\gamma} \cos\gamma \quad (6)$$

where

$$\dot{V} = \text{acceleration along flight path}$$

$$\dot{\chi} = \text{turn rate}$$

$$\dot{\gamma} = \text{rate of change of climb angle}$$

When analytical expressions for x, y, and z as functions of time are available then, of course, equations (1) - (6) are not required. This situation does not always arise, and, as will be demonstrated later, it is often easier to specify the flight velocity, the turn rate, and the altitude as functions of time, so that

$$\dot{\chi} = f_1(t) \quad (7)$$

$$z = f_2(t) \quad (8)$$

$$V = f_3(t) \quad (9)$$

By integrating equation (7) the track angle χ is found as a function of time. The z-axis component of velocity and acceleration can be found directly by differentiation of equation (8). Rearranging equation (3) gives

$$\gamma = -\sin^{-1} \left[\frac{\dot{z}}{V} \right] \quad (10)$$

and by differentiation

$$\dot{\gamma} = -\frac{\ddot{z}V - \dot{V}\dot{z}}{V^2 \cos \gamma} \quad (11)$$

As the velocity, V is also expressed as a function of time, equation (9), it is possible, using equations (1), (2), (4), (5), find the other component velocities and accelerations. Hence, any manoeuvre can be fully defined given the functions (7) - (9). The form these functions take depends on the geometry of the manoeuvre, as the examples in section 3 will show.

2.2 Load Factors

The most common approach adopted when attempting to assess the severity of a manoeuvre is to examine the load factor. It is intended here to refer to a 'flight-path load-factor' which is derived from the 'specific-force' of the manoeuvre, that is, the force per unit mass required to balance gravity and produce the flight path acceleration. This leads to the definition of the flight path load factor, n_{fp} according to

$$n_{fp} = \frac{1}{g} \sqrt{(\ddot{x}^2 + \ddot{y}^2 + (\ddot{z} - g)^2)} \quad (12)$$

It is also of interest to identify the two basic components of this force - the tangential component, n_t , for measuring the specific force along the flight path and the normal component, n_p associated with the curvature of the flight path

$$n_t = \frac{\dot{x}\ddot{x} + \dot{y}\ddot{y} + \dot{z}(\ddot{z} - g)}{g\sqrt{\dot{x}^2 + \dot{y}^2 + \dot{z}^2}} \quad (13)$$

$$n_p = \sqrt{n_{fp}^2 - n_t^2} \quad (14)$$

Having outlined the general approach to modelling manoeuvres, the following section shows the application of this methodology in developing mathematical models some specific manoeuvres.

3. Examples of Specific Manoeuvres

3.1 The Hurdle-hop Manoeuvre

As mentioned previously, the Hurdle-hop manoeuvre, shown in Figure 2, is used for obstacle avoidance in NOE flight where the helicopter has to clear an obstacle of height, h , then return to its original altitude. Here it is assumed that the total distance covered is s , and that the obstacle is at the midway point. In order to develop a mathematical representation of this manoeuvre it is necessary to express turn rate, altitude and velocity as functions of time. Since the Hurdle-hop manoeuvre is performed in the x - z plane (i.e. in two dimensions), there is no turn rate leaving only the flight velocity and altitude to define. It is important to consider the required flight path continuity before selecting the functions for altitude and flight velocity. It is not unreasonable to impose the condition that at the entry and the exit from the manoeuvre the flight path should correspond to a level trimmed flight state. Considering first the flight velocity, this implies constant velocity at the entry to and exit from the manoeuvre, and no acceleration at these points. Further, if it is assumed that the velocity at the entry and exit is the same, V_1 , and that a velocity V_2 is reached at the obstacle, then the velocity-defining function has to satisfy five boundary conditions as shown

$$\begin{aligned} \text{i) } t = 0, \quad V &= V_1, \quad \dot{V} = 0 \\ \text{ii) } t = t_m/2, \quad V &= V_2 \\ \text{iii) } t = t_m, \quad V &= V_1, \quad \dot{V} = 0 \end{aligned}$$

and the simplest appropriate analytical function becomes a fourth order polynomial, which can be shown to be of the form

$$V(t) = 16 \left[\left(\frac{t}{t_m} \right)^4 - 2 \left(\frac{t}{t_m} \right)^3 + \left(\frac{t}{t_m} \right)^2 \right] (V_2 - V_1) + V_1 \quad (15)$$

where t_m is the time taken to complete the manoeuvre. The altitude function is similarly defined by considering the required conditions at entry and exit. The simplest set of boundary conditions are

$$\begin{aligned} \text{i) } t = 0, \quad z &= 0, \quad \dot{z} = 0, \quad \ddot{z} = 0 \\ \text{ii) } t = t_m/2, \quad z &= -h \\ \text{iii) } t = t_m, \quad z &= 0, \quad \dot{z} = 0, \quad \ddot{z} = 0 \end{aligned}$$

As well as giving the correct height change, setting the first derivative to zero ensures level flight, equation (10), and the trim state is ensured by setting the second derivative to zero. As there are seven boundary conditions, a sixth order polynomial is the simplest suitable function, and the altitude-defining function is found to be

$$z(t) = \left[64 \left(\frac{t}{t_m} \right)^6 - 192 \left(\frac{t}{t_m} \right)^5 + 192 \left(\frac{t}{t_m} \right)^4 - 64 \left(\frac{t}{t_m} \right)^3 \right] h \quad (16)$$

It is apparent from equations (15) and (16) that if the height, h , velocities, V_1 and V_2 and time t_m are specified, then the manoeuvre may be defined, however, it is much more convenient to specify the manoeuvre distance, s , the height and the velocities, then calculate the manoeuvre time. This is possible by first noting that

$$V = \sqrt{\dot{x}^2 + \dot{y}^2 + \dot{z}^2} \quad (17)$$

and, in the case of a Hurdle-hop flown in the direction of the earth x -axis,

$$s = \int_0^{t_m} \sqrt{V^2 - \dot{z}^2} dt \quad (18)$$

This equation can be solved numerically to obtain the manoeuvre time t_m given s , h , V_1 and V_2 . Other manoeuvres in the x - z plane can be defined in the same manner, indeed, the method of choosing boundary conditions then fitting a suitable polynomial can be adapted to suit other velocity, altitude or turn rate functions as will become apparent.

3.2 Linear Repositioning Manoeuvres

There are three linear repositioning manoeuvres commonly used in NOE flight : the Quick-hop, Figure 6, the Side-step, Figure 3, and the Bob-up, Figure 4. In each case the helicopter begins and ends the manoeuvre in a trimmed hover flight state, translating over a specified linear distance in between. If it is assumed that the helicopter's body x -axis is in line with the earth x -axis, then the Quick-hop manoeuvre is flown along the earth x -axis, the Side-step manoeuvre is flown along the y -axis, and the Bob-up is flown along the z -axis. It is then apparent that the same definition may be used, with minor modifications, for each type of manoeuvre. As the manoeuvres are flown without deviation from a straight line there can be no turn rate, and the component velocity along the appropriate axis is simply equal to the flight velocity, so that

$$\begin{aligned} \text{Quick - Hop} & : \dot{x}(t) = V(t) \\ \text{Side - Step} & : \dot{y}(t) = V(t) \\ \text{Bob - Up} & : \dot{z}(t) = V(t) \end{aligned}$$

To define the manoeuvre it is therefore sufficient to specify the flight velocity function, the first stage being to consider the boundary conditions which must be applied. As the manoeuvre is to begin and end in a trimmed hover flight state the four boundary conditions of zero velocity and acceleration at the entry and exit must be applied. During the manoeuvre the helicopter accelerates to some maximum velocity, V_{max} , then decelerates back to the hover. For convenience it is assumed that the maximum velocity is reached midway through the manoeuvre ($V=V_{max}$ at $t=t_m/2$). This latter condition may be applied at other than the mid time, of course, but flight data has justified the choice made here. The mid way condition and the four entry and exit conditions gives a fourth order polynomial as the simplest analytical function :

$$V(t) = \left[16 \left(\frac{t}{t_m} \right)^4 - 32 \left(\frac{t}{t_m} \right)^3 + 16 \left(\frac{t}{t_m} \right)^2 \right] V_{max} \quad (19)$$

As in the Hurdle-hop, it is more realistic to specify the translational distance, s , over which the manoeuvre is to be performed rather than the time taken. Integrating the velocity over the duration of the manoeuvre gives

$$t_m = \frac{15s}{8V_{max}} \quad (20)$$

Hence, by simply specifying a translational distance, s , and the maximum velocity to be achieved, V_{max} , it is possible to calculate the manoeuvre time, t_m from equation (20), then by integration of equation (19) the flight path co-ordinates can be found.

3.3 The Level Turn Manoeuvre

This example differs from the previous two in that here it is necessary to define a turn rate function. The most basic turn would simply consist of a circular arc which, noting that

$$\dot{\chi}(t) = \frac{V(t)}{R_c} \quad (21)$$

where R_c is the radius of the circular flight path, would give a constant turn rate - assuming constant velocity. Using a circular arc poses the problem of continuity at the entry and exit sections of the manoeuvre where the circular flight path (with a finite value of turn rate) joins linear sections (with zero turn rate). This problem can be overcome by imposing transient sections on the turn at the entry and exit points as shown in Figure 9, where the circular section and exit transients are reached after t_1 and t_2 seconds respectively. The resulting flight path is shown in Figure 10 where the broken line indicates the equivalent circular flight path of radius R_e , whilst R_c is the radius of the circular section, and χ_1 , χ_2 , and χ_3 are the track angles swept out in the entry transient, circular section, and exit transients respectively. It is convenient to

define a parameter, k , which indicates the proportion of the manoeuvre spent in these transients, so that

$$\chi_1 = k\chi_e \quad \chi_2 = (1 - 2k)\chi_e \quad \chi_3 = k\chi_e \quad (22)$$

where χ_e is the track angle at the exit of the manoeuvre. The whole manoeuvre is assumed to be flown at a constant altitude (i.e. $z(t) = \text{constant}$), and as in the previous examples, it is assumed that the manoeuvre is initiated from a steady, level flight state. If a turn rate time-history of the form given in Figure 9 is desired, then the manoeuvre must be performed at constant velocity, i.e. $V_1 = V_2$, and it is this case which will be discussed here. The more general case which allows velocity to be varied through the manoeuvre is discussed in Reference 11. As both velocity and altitude are held constant, the manoeuvre may be defined simply by specifying an appropriate function for the turn rate. Referring to Figures 9 and 10, it is evident that there are three distinct sections in the manoeuvre (entry transient, circular arc, and exit transient), and it follows that the turn rate must be specified individually in each.

a) The Entry Transient

As in previous examples, the starting point is to consider the required conditions at the beginning and end of the section. At the start of the manoeuvre a steady trim condition is required which gives a zero turn rate and acceleration condition at the entry to the manoeuvre. At time t_1 where the circular section is reached, the turn rate has increased to some maximum value dependent on the velocity $V_c (=V_1 = V_2)$ and radius of the circular section, R_c so that the boundary conditions, referring to Figure 9, are given by

$$\begin{aligned} \text{i) } t = 0, \quad \dot{\chi} &= 0, \quad \ddot{\chi} = 0 \\ \text{ii) } t = t_1, \quad \dot{\chi} &= \frac{V_c}{R_c} = \dot{\chi}_m, \quad \ddot{\chi} = 0 \end{aligned}$$

A cubic polynomial is the simplest appropriate function, and applying these boundary conditions, it is found to be of the form

$$\dot{\chi}(t) = \left[-2 \left(\frac{t}{t_m} \right)^3 + 3 \left(\frac{t}{t_m} \right)^2 \right] \dot{\chi}_m \quad (23)$$

Noting that the track angle swept out in the transient can be found by integrating the turn rate over the time t_1 ,

$$\chi_1 = k\chi_e = \int_0^{t_1} \dot{\chi}(t) dt \quad (24)$$

the time in the entry transient, t_1 , is found to be

$$t_1 = \frac{2k\chi_e}{\dot{\chi}_m} \quad (25)$$

b) The Circular Section

Turn rate is constant in this section, and, as in equation (24) by integration, the time t_2 is found to be

$$t_2 = t_1 + ((1 - 2k)\chi_e)/\dot{\chi}_m \quad (26)$$

c) The Exit Transient

In this section the turn rate boundary conditions are defined as

$$\begin{aligned} \text{i) } t = t_2, \quad \dot{\chi} &= \dot{\chi}_m, \quad \ddot{\chi} = 0 \\ \text{ii) } t = t_m, \quad \dot{\chi} &= 0, \quad \ddot{\chi} = 0 \end{aligned}$$

This gives the required turn rate at the entry to the transient, and a straight line flight condition at the exit. As in the entry transient, a cubic polynomial is used to satisfy these conditions. The polynomial is of the form

$$\dot{\chi}(t) = \left[2t^3 - 3(t_m + t_2)t^2 + 6t_m t_2 t - (3t_m - t_2)t_2^2 \right] \left[\frac{\dot{\chi}_m}{(t_m - t_2)^3} \right] + \dot{\chi}_m \quad (27)$$

Integration of this turn rate function between t_2 and the manoeuvre time t_m yields

$$t_m = t_2 + \frac{2k\chi_e}{\dot{\chi}_m} \quad (28)$$

It is apparent that if the constant velocity, V_c , the transient fraction, k , the exit track angle, χ_e and radius of the circular section R_c were specified, then it would be possible to calculate all of the polynomial coefficients and times, hence the manoeuvre could be fully defined. This will not however, allow any control over the exit position. The most convenient way to specify the manoeuvre is by considering the equivalent circular path, Figure 10, and specifying the equivalent radius, R_e , hence ensuring that the required exit position is reached. An iterative scheme to calculate the circular arc radius, R_c , is required to achieve this: an initial guess of the value of R_c is made (based on the input value of R_e), the turn rate and component times through the manoeuvre are then calculated using equations (23-28), and by integrating equations (1) and (2) with $\gamma=0$, the exit co-ordinates corresponding to the current value of R_c are obtained.

$$x_e = R_e \sin\chi_e = \int_0^{t_m} V(t)\cos\chi(t) dt \quad (29)$$

$$y_e = R_e (1 - \cos\chi_e) = \int_0^{t_m} V(t)\sin\chi(t) dt$$

The value of R_c is adjusted until the appropriate exit co-ordinates are reached.

3.4 The Pull-up/Push-Over Manoeuvre

The description of this manoeuvre is taken from Ref. 3. It rests on a definition of the load factor as a function of time and for clarity uses the specific values from Ref.3 although they are readily generalised. Starting from a level trimmed flight condition, at a given airspeed, a load factor of at least $2g$ is attained within one second of the start of manoeuvre. It is maintained for at least one second, before a transition to a push over of not greater than $0g$. The transition is to take less than two seconds, and the push over sustained to achieve the airspeed at manoeuvre entry. The manoeuvre is longitudinal and so χ may be set to zero. Figure 9 shows a reasonable interpretation of this description as a normal load factor profile. Initially the load factor, n_p , measured in units of g , is unity, between the initial time $t=0$ and time $t=t_1$, (1 second) a smooth transition to load factor of 2 is made by a polynomial of degree 5 satisfying

$$\begin{aligned} \text{i) } t = 0, \quad n_p &= 1, \quad \dot{n}_p = 0, \quad \ddot{n}_p = 0 \\ \text{ii) } t = t_1, \quad n_p &= 2, \quad \dot{n}_p = 0, \quad \ddot{n}_p = 0 \end{aligned}$$

It remains constant at a value of 2 until time $t=t_2$ (2 sec.) where begins a similar smooth transition to a zero load factor achieved at $t=t_3$ (4 sec.) satisfying

$$\begin{aligned} \text{i) } t = t_2, \quad n &= 2, \quad \dot{n}_p = 0, \quad \ddot{n}_p = 0 \\ \text{ii) } t = t_3, \quad n &= 0, \quad \dot{n}_p = 0, \quad \ddot{n}_p = 0 \end{aligned}$$

The zero value is maintained until time $t=t_4$, and a smooth transition is made back to unity load factor at $t=t_5$.

$$\begin{aligned} \text{i) } t = t_4, \quad n &= 0, \quad \dot{n}_p = 0, \quad \ddot{n}_p = 0 \\ \text{ii) } t = t_5, \quad n &= 1, \quad \dot{n}_p = 0, \quad \ddot{n}_p = 0 \end{aligned}$$

The values of t_4 and t_5 remain to be chosen, since they are not explicitly specified in the description of the manoeuvre. The return to unity load factor from its zero value is not intended to be a demanding part of the task, so we have halved its severity compared to other transitions and set its duration at 2 seconds, therefore $t_5-t_4=2$. The value of t_5 is determined by recalling that the airspeed should have returned to its original value at the end of the manoeuvre, therefore t_5 is adjusted until the value of the airspeed at t_5 is equal to that at the start of the manoeuvre. The load factor in terms of climb angle γ and airspeed, V , may be obtained from (12), (13) and (14) as

$$n_p = \frac{V\dot{\gamma}}{g} + \cos\gamma \quad (30)$$

which when rearranged according to

$$\dot{\gamma} = \frac{g(n_p - \cos\gamma)}{V} \quad (31)$$

can be solved for g once the airspeed V is known throughout the manoeuvre. There is little information about the variation of airspeed, and directly imposing a predetermined profile for it does not seem to be in the spirit of the task - although it can easily be done if required. The view taken in the current work is to assume that during the manoeuvre any gain in potential energy is balanced by a loss of translational kinetic energy, so that as the helicopter gains height during the pull up, the airspeed reduces, and correspondingly the loss of height in the latter stages of the push over will recover the lost airspeed. The equation expressing this balance is

$$\dot{V} = -g\sin\gamma \quad (32)$$

The differential equations (31) and (32) are solved subject to the initial conditions $V(0)=V_{\text{trim}}$ (V_{trim} being the trim airspeed at manoeuvre entry) and $\gamma(0)=0$. The equations are solved with particular choice of t_5 , and t_5 is adjusted until the exit conditions $V(t_5)=V_{\text{trim}}$ is satisfied. Figures 12 and 13 show the profiles of flight path angle and airspeed which result from the load factor of Fig. 11.

From airspeed and climb angle, the flight path coordinates are easily obtained from equations (4) and (6), noting that the track angle, χ , is zero, which are conveniently integrated using the same scheme as (30) and (31).

From the examples discussed in detail, above, it is apparent that any manoeuvre may be specified by the use of simple polynomial expressions for the key parameters of altitude, turn rate, flight velocity and load factor. The lowest order of polynomial compatible with acceptable derivative continuity has been used. In inverse simulation, the continuity that must be applied depends on the order of the embedded mathematical model. In the current work a requirement for continuous accelerations is generally found to be sufficient, but one exception is the additional continuity attached to the load factor profile in the pull-up/push-over manoeuvre. An additional order of continuity was found to be necessary to obtain rapid convergence of the iteration involved in the manoeuvre algorithm.

If required, higher order continuity can be achieved by increasing the order of the polynomial, and the effect this has on the manoeuvre profile is discussed in section 6. Before this is done, the validity of the mathematical representations is considered, by comparison with data from flight tests.

4. Validation of Manoeuvres Against Flight Data

Validation is an important part of any modelling exercise. In this case, flight path data from agility flight trials has been used to validate certain of the modelled trajectories by direct comparison. The flight trials were performed at the Royal Aerospace Establishment, Bedford, using a Westland Lynx helicopter and involved tests on a series of different manoeuvres. During the trials, the aircraft's states and controls are measured and recorded onboard, whilst its position relative to the ground is measured and recorded by a kinetheodolite tracking system. The positional co-ordinates are recorded at constant time intervals, and using numerical differentiation it is possible to determine the earth axis component velocities of the helicopter, and hence, using equation (17), the flight velocity can be determined. This information is now used to compare the flight paths from actual helicopter manoeuvres with those derived numerically in Section 3.

The first comparison made is of data measured in tests involving two linear repositioning manoeuvres: Side-step and Quick-hop [13]. In these trials, the pilot's objective was to fly the helicopter, from a hover condition, over a specified step length, then back to the hover again as aggressively as possible, whilst maintaining a constant height. This is equivalent to the definitions of the Quick-hop and Side-step discussed in Section 3.2. By examining the velocity profile from the flight trial the maximum velocity attained, V_{max} , was established and as the step size, s , is also known, there is enough information to produce a mathematical representation of the manoeuvre. In this case little information will be obtained by comparing flight paths as they are simply straight lines. Instead, as the linear repositioning manoeuvres are defined from their velocity profile, it is more appropriate to compare these. Figure 14 shows comparisons of the fourth order polynomial used to specify the flight velocity and the actual velocity from both Side-step (Fig. 14a) and Quick-hop (Fig. 14b) flight trials. In both cases it is apparent that the basic form of the helicopter's velocity profile is reproduced by the quartic function, however, there are small differences in the slope of the curve which will produce slightly different acceleration profiles. It is also noticeable that the assumption of maximum velocity at the mid point of the manoeuvre is valid.

The second set of data presented here was measured during trials aimed at studying the agility of helicopters in turning flight [14]. In these trials the pilots were instructed to perform turns of a specific radius by using markers on the ground for visual cues. The pilot was also instructed to maintain both a constant height and flight velocity through the manoeuvre. As with the linear repositioning manoeuvres this appears to be suitable for comparison with the turns defined in Section 3.3. Flight path data (positional co-ordinates) were obtained for a flight test where the pilot was instructed to fly a 400ft (122m) left hand turn at a constant

velocity of 70 knots. From the data it was apparent that the pilot had actually flown a turn of radius 118m, shown as a series of triangular symbols on Figure 15. Thus the equivalent radius of the modelled turn, R_e is taken to be 118m, the exit track angle χ_e , is 90 degrees, and the constant flight velocity, V_c is 70 knots, leaving only the transient factor, k , to be determined. The most appropriate value of k is determined by varying it and comparing the resulting flight path with that measured in the flight trial. This is shown in Figure 15 where two modelled flight paths ($k=0.1$ and 0.2) are plotted alongside the measured flight path. It is clear that the value of 0.2 for k is the more suitable, indeed this gives a very good comparison between the actual and modelled flight paths.

The comparisons with flight data suggest that the modelling approach adopted has given valid results for the examples given above. Without the availability of more flight data, particularly for height change manoeuvres such as the Hurdle-hop and Pull-up/push-over, it is difficult to give a conclusive statement as to whether the techniques will be universally valid. The results so far are, however, encouraging.

5. Methods of Grading Manoeuvres

One result of a precise definition of a manoeuvre is that it is possible to assess the ability of a helicopter to perform the manoeuvre. This assessment can prove useful on three levels. Firstly, and the most basic consideration, is whether the installed power can actually deliver the accelerations and decelerations of the helicopter inertia that the flight path requires. The second factor to be considered is whether the aerodynamic design of the helicopter will release that performance for use in executing the manoeuvre. Finally, an assessment of handling qualities will determine the ease with which the pilot can achieve the specified task.

Relating these three levels to a simulation environment it is clear that the first of these questions can be approached simply from a definition of the flight path. To supply the answers to the second, a suitable helicopter model must be incorporated into the simulation study. As yet the third consideration, that of handling qualities, is beyond the scope of non-piloted simulations and even stretches current flight simulator technology. Accordingly, in this section, attention is confined to the first two questions: grading-criteria using flight path information alone and then subsequently with a helicopter model in addition.

5.1 Flight Path Load Factor

The application of equation (12) to any flight path definition allows the time history of the flight path load factor to be determined. The significance of this is that the peak load factor can be found hence giving a simple measure of whether a helicopter is capable of flying the defined manoeuvre without exceeding design limits. This is illustrated in Figure 16 where the flight path load factor is for three similar manoeuvres is plotted. The three manoeuvres represent a single flight path (a hurdle-hop of distance 400m and obstacle height 25m) flown at different constant velocities. The effect this has on peak load factor is clearly visible.

5.2 Thrust Factor

The introduction of a mathematical model of a helicopter enables the flight path to be used to drive an inverse simulation. The results of the simulation incorporate both aerodynamic effects and rotational inertias and their influence can be observed in the comparison of n_{fp} and the thrust factor, n_{Th} , which is defined as the ratio of thrust to weight coefficients.

$$n_{Th} = \frac{C_T}{C_w} \quad (33)$$

$$C_T = \frac{T}{\rho(\Omega R)^2 \pi R^2} \quad C_w = \frac{mg}{\rho(\Omega R)^2 \pi R^2}$$

Figure 17 shows such a comparison for a hurdle-hop manoeuvre ($s=400m$, $h=25m$ and $V=80$ knots, as in the example above) where the thrust factor throughout the manoeuvre has been calculated using a mathematical model of a Westland Lynx helicopter in the inverse simulation. At the entry and exit portions of the manoeuvre there is good correlation between the two plots. This is to be expected as in these regions the angle of attack of the helicopter fuselage is low, hence the aerodynamic forces and moments are also low. During the manoeuvre, as the angle of attack increases and the aerodynamic forces and moments become significant, there is a noticeable difference between the flight path load factor and the thrust factor.

5.3 Collective Factor

The closest that this type of analysis can approach pilots' control actions is to generate control movements from the inverse simulation and attach suitable criteria to them. In the spirit of the discussion above, it is appropriate to relate the thrust factor to the collective displacement. Defining a collective factor, n_{θ_0} as

$$n_{\theta_0} = \frac{\theta_0}{\theta_{0_{\text{trim}}}} \quad (34)$$

where θ_0 and $\theta_{0_{\text{trim}}}$ are the main rotor collective pitch angle and its value at the trimmed entry to the manoeuvre respectively, it is possible to compare the previously defined flight path load and thrust factors with one representing what the pilot actually has to do to fly the manoeuvre. In Figure 19 the same Hurdle-hop manoeuvre can be used ($s=400\text{m}$, $h=25\text{m}$, $V=80$ knots), and data for a Westland Lynx helicopter was used in the inverse simulation. A major influence in the discrepancy is the inflow through the rotor and the collective ratio varies significantly from the thrust factor. Gradings of manoeuvre/helicopter combinations based on criteria attached to the collective ratio go some way to measuring the control movements demanded of the pilot by the particular helicopter configuration. Comparisons can be made for a single helicopter over a range of manoeuvres, or a variety of helicopter configurations over a series of manoeuvres.

6. The Effect of Polynomial Order on Manoeuvre

It is apparent from Section 3 that the methods used to create mathematical representations of helicopter flight paths rely to a large degree on the use of polynomial functions. As a general rule, the lowest order polynomial which gives a constant velocity and zero acceleration state at the entry and exit points was chosen. It is of course possible to choose polynomials of greater or lesser order, and the effect of doing so is discussed in this section.

The example taken is of the Hurdle-hop manoeuvre. In Section 3.1 it was shown that a 6th order polynomial gave the required "trim" continuity at entry and exit for the Hurdle-hop. If the zero acceleration requirement is neglected, two boundary conditions are lost, and a quartic polynomial is sufficient to define the manoeuvre. Another alternative is to apply the further conditions that the rate of acceleration (often referred to as "jerk") is required to be zero at entry and exit, the extra two boundary conditions giving an 8th order polynomial. The resulting flight paths are shown in Figure 19 along with the original 6th order polynomial trajectory. As the order of the polynomial is increased to produce higher order continuity at the entry and exit points, it is apparent that the flight path has become flatter at these regions. The flight path then has to have higher curvature in order to give the correct height change. The consequence this has on the maximum flight path load factor is shown in Figure 20. There are two points of interest concerning this plot. Firstly, the quartic polynomial flight path gives a non-unity load factor at entry and exit - underlining the fact that the helicopter would not be in a trim state at these points. Further, the result of this definition would be discontinuities in

acceleration at the entry and exits rendering this representation unsuitable. The other point of note is that as the order of the polynomial is increased the maximum flight path load factor also increases. It is evident that whichever of the above criteria for grading the manoeuvres were applied to the higher order polynomial path, the result would be a higher severity factor.

In Section 4 comparisons were made between flight data and modelled flight paths. In each case good correlation was achieved using the minimum order polynomial for a trim state at entry and exit. In this section it is shown that other polynomials may also give these requirements but with important consequences on the severity of the manoeuvre. Without the benefit of flight data for the Hurdle-hop manoeuvre it is impossible to say which order of polynomial gives the most accurate representation. However, in the light of the results from the validation exercise performed in Section 4, the use of the minimum order polynomial (in this case of order 6) in the first instance should give a good mathematical model of the flight path.

7. Conclusions

The following conclusions can be drawn from the research carried out in the field of manoeuvre modelling and classification presented in this paper.

1. A need for mathematical representations and classification of helicopter manoeuvres for use with inverse simulation packages, certification and handling qualities studies has been identified. Of these three applications, inverse simulation is currently the most demanding, since a full numerical profile of the flight path being required.
2. Techniques have been demonstrated for defining manoeuvres in terms of a mathematical statement of their trajectory. Some of the descriptions are formulated as explicit expressions, others have an algorithmic content.
3. There are several ways to express flight trajectories; the choice depends on the convenience of formulation since kinematically they are equivalent. The most useful options have used
 - (a) Earth fixed axes x,y,z for position, velocity or acceleration.
 - (b) Airspeed, turn rate and altitude. (V, χ, h)
 - (c) Airspeed, turn rate and climb angle. (V, χ, γ)

4. The most convenient approach to adopt when modelling manoeuvres is to use simple polynomial curves to represent key kinematic quantities such as displacements or velocities. There is good agreement between the assumed polynomial form and flight data for the manoeuvres where data is available.
5. Having examined the effect of altering the order of the defining polynomial, it can be concluded that there is no observed advantage in using a higher order of polynomial than that which meets the essential entry and exit conditions.
6. Manoeuvres can be graded in terms of their severity. In order to do this a flight path load factor has been defined as being the specific force required to perform the manoeuvre.

Finally, a request should be made to those concerned with compiling performance and handling qualities requirements. When manoeuvres are specified, the needs of simulation studies should be borne in mind. While there may be no need to go to the extent of defining precise trajectories, there should be a complete statement of the required entry and exit conditions, and supplementary information about the conditions to be applied at significant intermediate stages of the manoeuvre. If this is done then the combination of manoeuvre modelling and inverse simulation can form a powerful supplement to a flight test programme for evaluating manoeuvre performance.

8. References

1. Federal Aviation Regulations, Part 29 - Airworthiness Standards : Transport Category Rotorcraft, 1974, U.S. Department of Transportation, Federal Aviation Administration.
2. Cerbe, T., Reichert, G. Optimisation of Helicopter Takeoff and Landing, Proceedings of the International Congress of the Aeronautical Sciences, 1988, Paper No. ICAS-88-6.1.2
3. Hoh, R.H., Mitchell, D.G., Aponso, B.L., Key, D.L., Blanken, C.L., Proposed Specification for Handling Qualities of Military Rotorcraft, Volume 1 - Requirements, USAAVSCOM Technical Report 87-A-4, May 1988.
4. Thomson, D.G., Bradley, R., Development and Verification of an Algorithm for Helicopter Inverse Simulation, Vertica, May 1990.

5. Thomson, D.G., Evaluation of Helicopter Agility Through Inverse Solution of the Equations of Motion, Ph.D. Dissertation, Department of Aeronautics and Fluid Mechanics, University of Glasgow, May 1987.
6. Thomson, D.G., Bradley, R. An Investigation of Flight Path Constrained Helicopter Manoeuvres by Inverse Simulation, Proceedings of the 13th European Rotorcraft Forum, Arles, France, September 1987.
7. Thomson, D.G., Bradley, R., An Investigation of Pilot Strategy in Helicopter Nap-of-the-Earth Manoeuvres by Comparison of Flight Data and Inverse Simulations, Proceedings of the Royal Aeronautical Society Conference: Helicopter Handling Qualities and Control, London, November 1988.
8. Bradley, R., Padfield, G.D., Murray-Smith, D.J., Thomson, D.G., Validation of Helicopter Mathematical Models, Transactions of the Institute of Measurement and Control, Volume 12, No. 4, 1990.
9. Padfield, G.D., A Theoretical Model of Helicopter Flight Mechanics for Application to Piloted Simulation, RAE TR 81048, April 1981.
10. Thomson, D.G., Bradley, R., Prediction of the Dynamic Characteristics of Helicopters in Constrained Flight, The Aeronautical Journal, December 1990.
11. Thomson, D.G., Bradley, R. Mathematical Representation of Manoeuvres Commonly Found in Helicopter Nap-of-the-Earth Flight, Department of Aeronautics and Fluid Mechanics, University of Glasgow, Internal Report, Aero. Report 8801, Feb. 1988.
12. Thomson, D.G., Bradley, R., The Use of Inverse Simulation for Conceptual Design Proceedings of the 16th European Rotorcraft Forum, September 1990.
13. Charlton, M.T., Padfield, G.D., Horton, Lt. Cdr, R.I., Helicopter Agility in Low Speed Manoeuvres, Paper 9.10, Proceedings of the 13th European Rotorcraft Forum Arles, France, September 1987.
14. Brotherhood, P., Charlton, M.T., An Assessment of Helicopter Turning Performance During Nap-of-the-Earth Flight, RAE Tech. Memo. FS(B) 534, January 1984

9. **Acknowledgements**

The authors wish to acknowledge the contribution of Dr G.D. Padfield of the Royal Aerospace Establishment, Bedford to this work, particularly in relation to the HELISTAB model and the flight data used in this study. This research was initially carried out as part of the Ministry of Defence Extra Mural Agreement 2048/39/XR/FS. Work is currently funded by the Royal Society under their 1983 Universities Research Fellowship scheme.

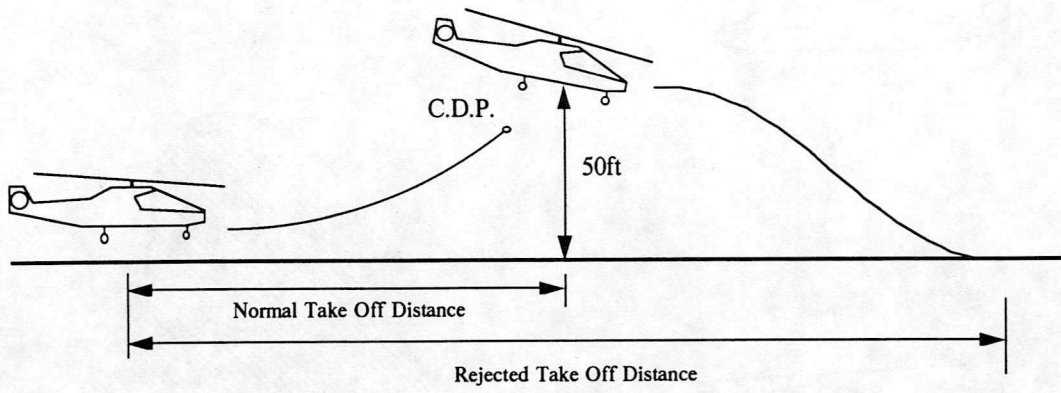


Figure 1 : Take-off Flight Path for FAA Regulations

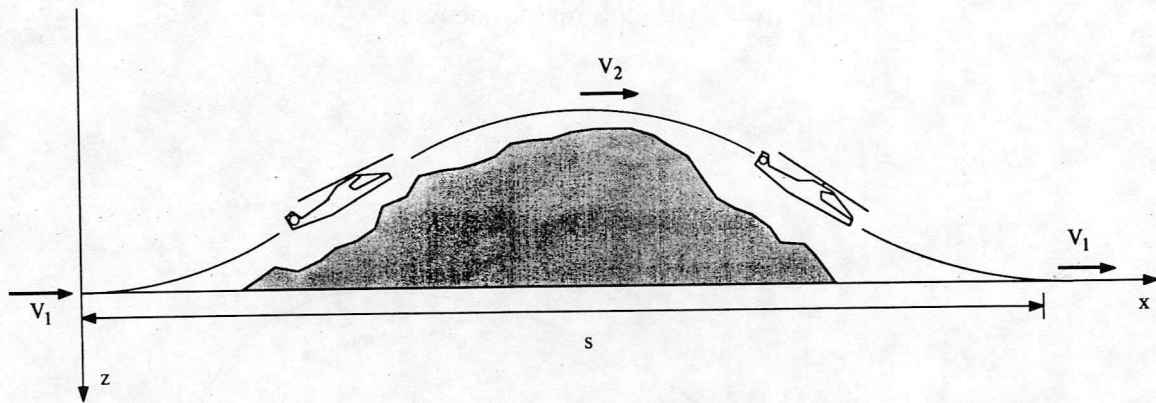


Figure 2 : The Hurdle-hop Manoeuvre

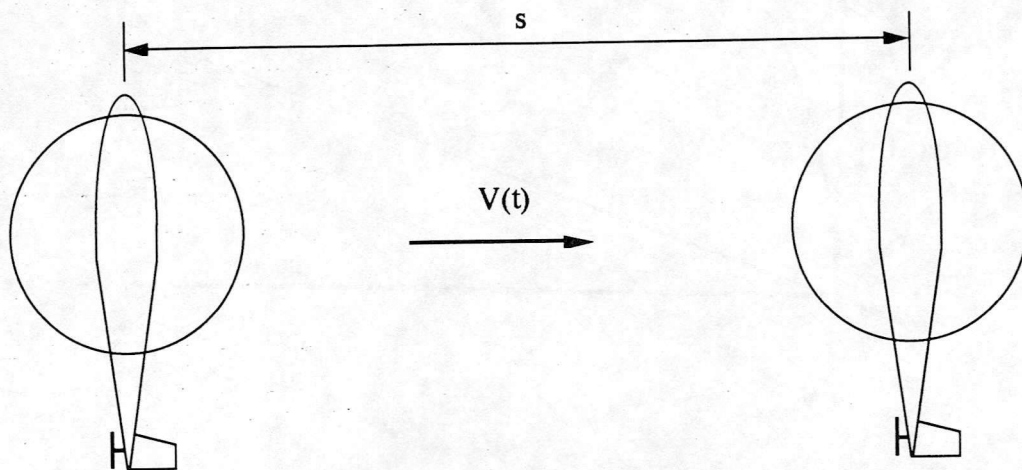


Figure 3 : The Side-step Manoeuvre

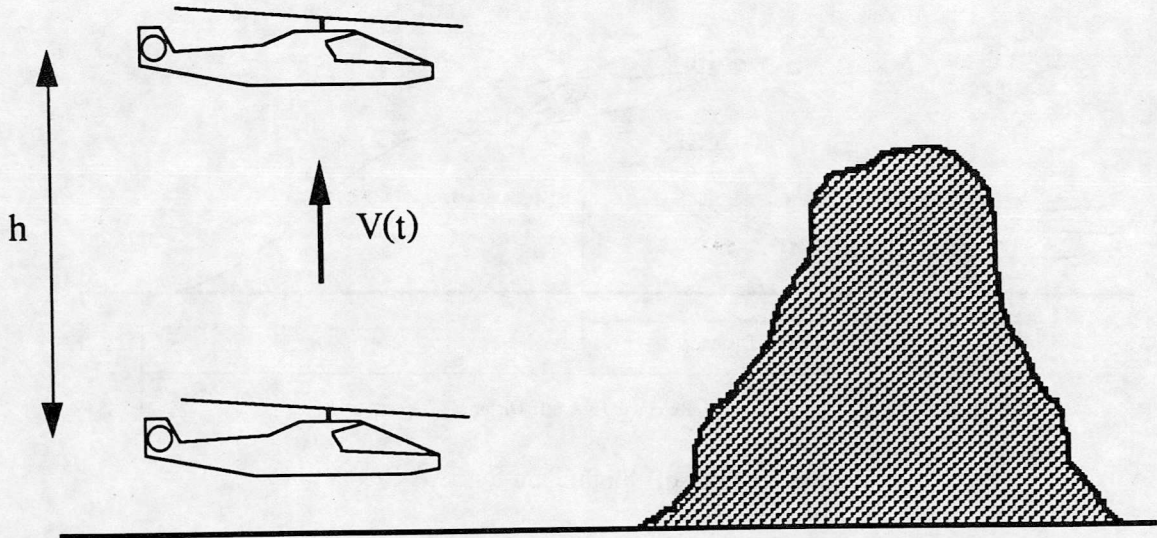


Figure 4 : The Bob-up Manoeuvre

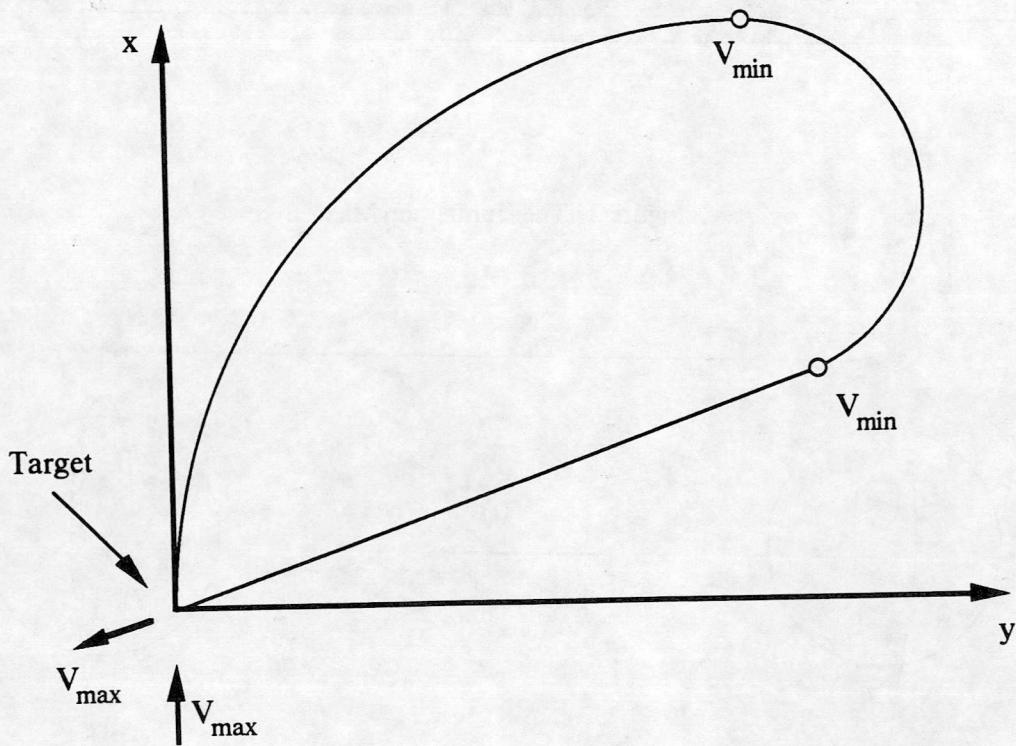


Figure 5 : The Tear-drop Turn Manoeuvre

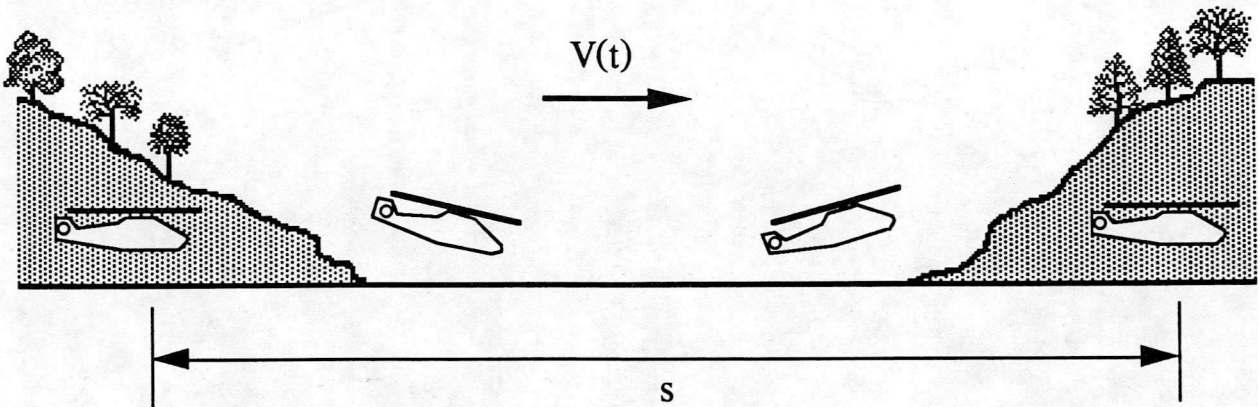


Figure 6 : The Quick-hop Manoeuvre

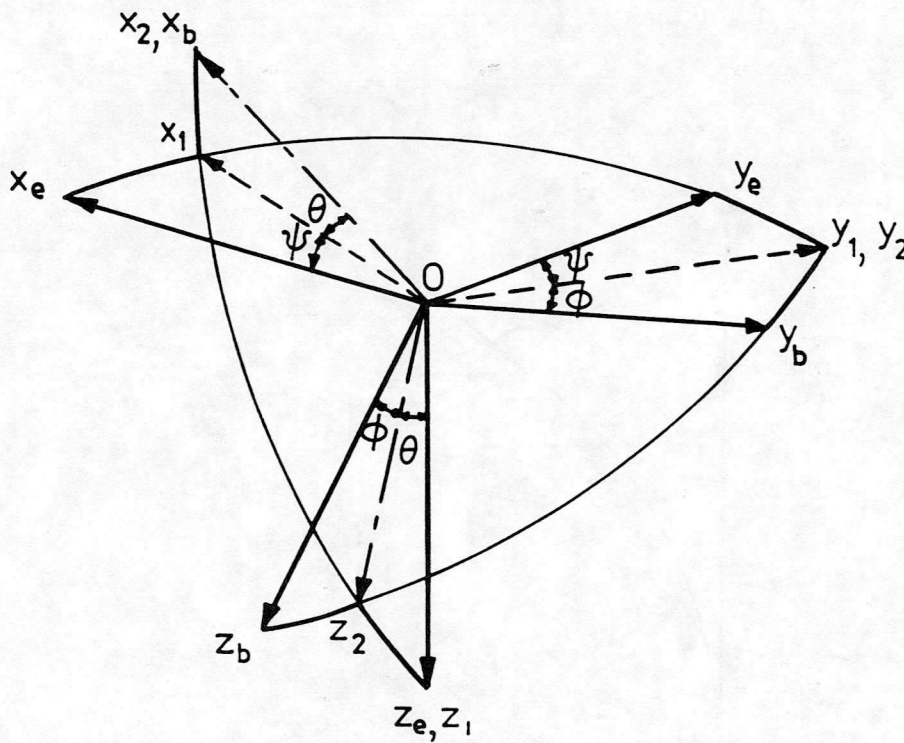
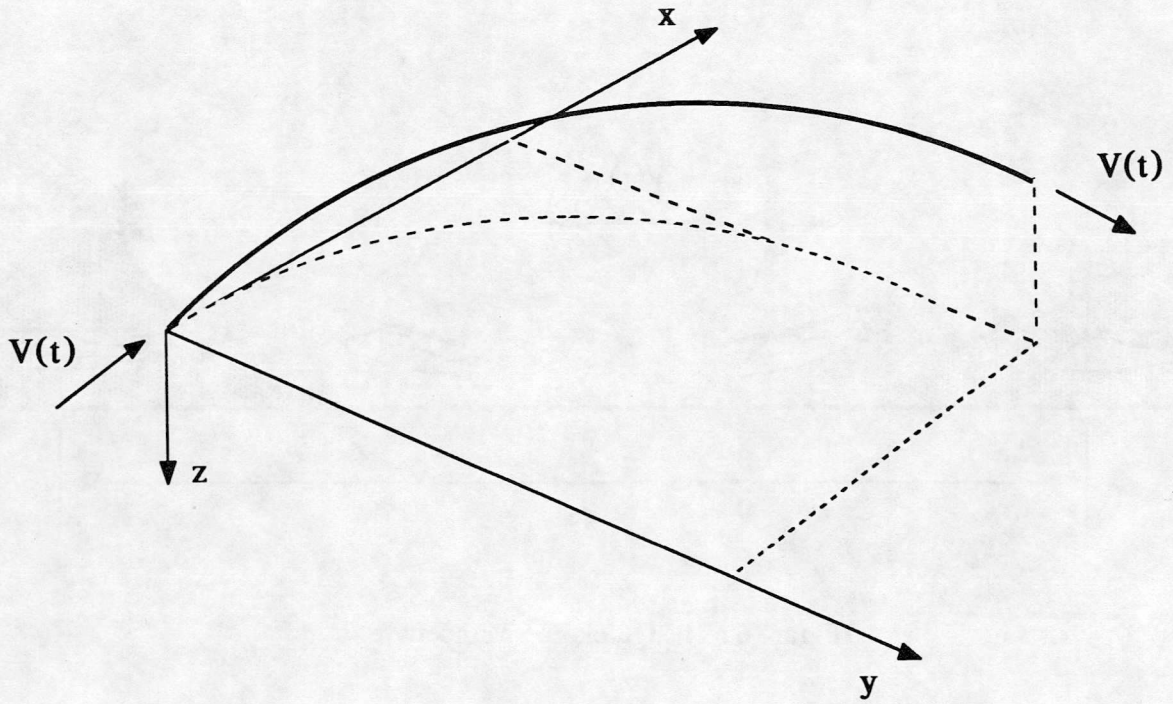
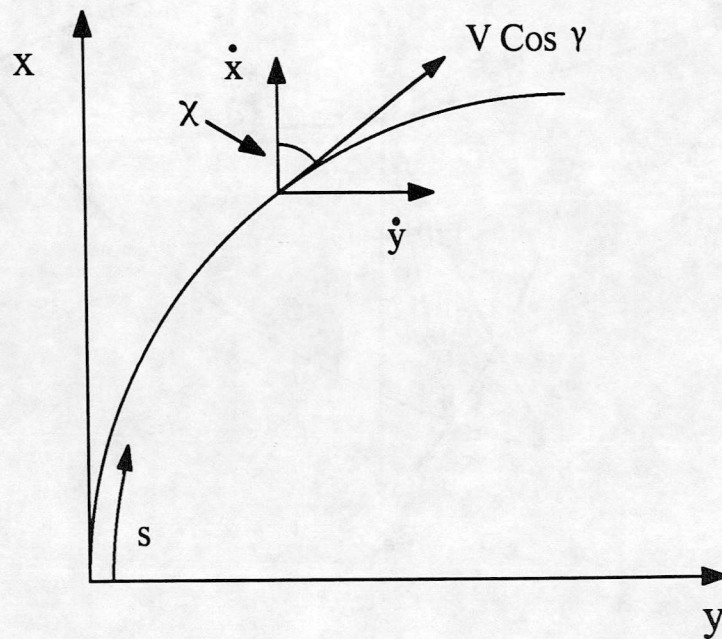


Figure 7 : Euler Angle Transformation Between Earth and Body Fixed Axes Systems

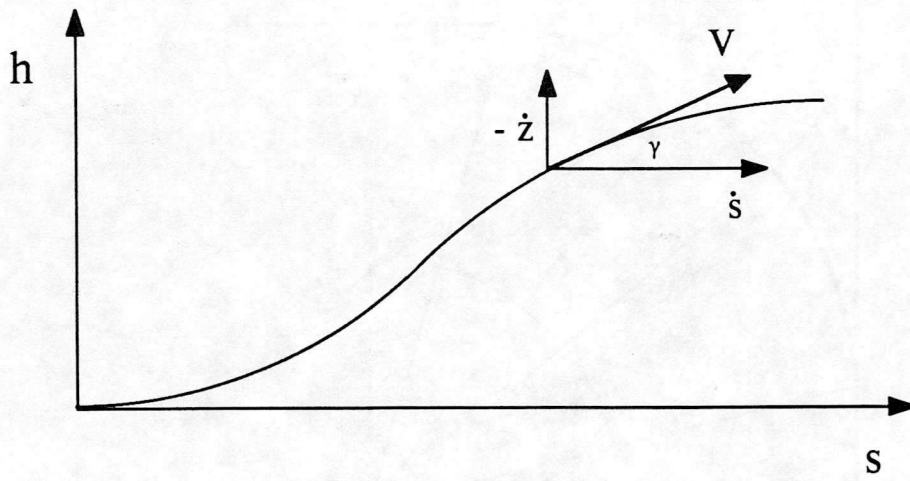


a) The 3-D Manoeuvre



b) The Track

Figure 8 : A General 3-Dimensional Manoeuvre



c) The Altitude

Figure 8 : Continued

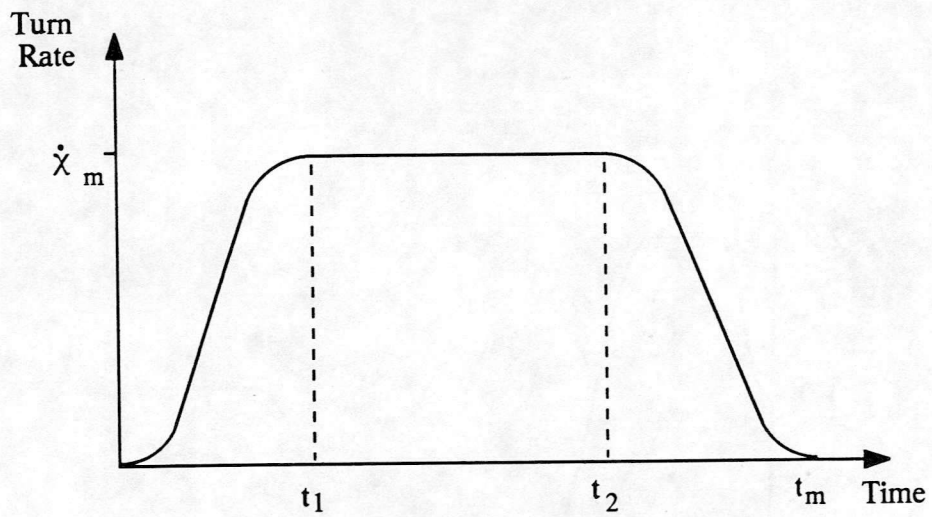


Figure 9 : Turn Rate in a Constant Velocity Level Turn Manoeuvre

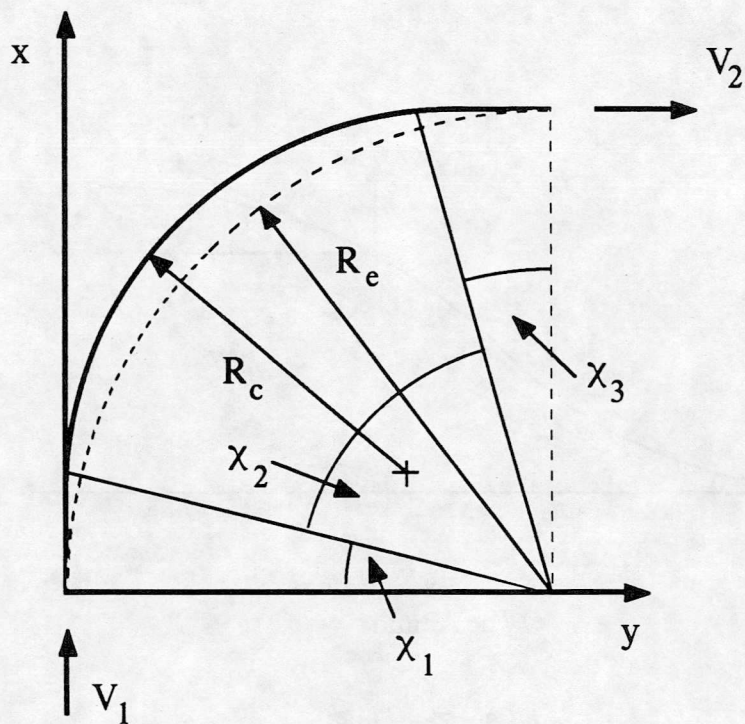


Figure 10 : The Level Turn Manoeuvre

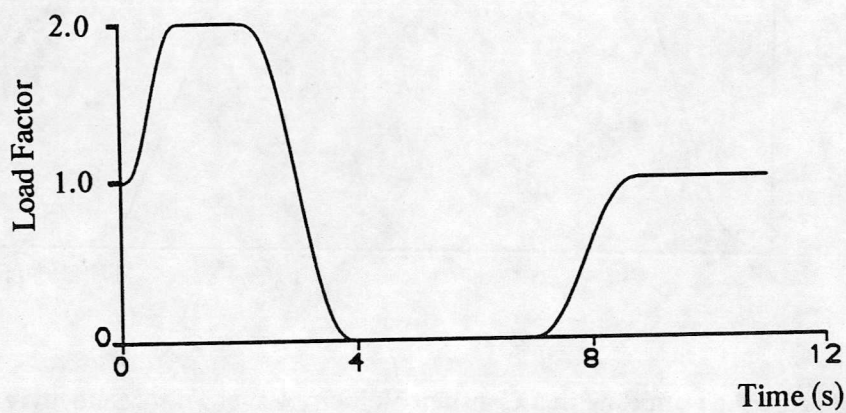


Figure 11 : Load Factor Distribution in Pull-up/Push-over Manoeuvre

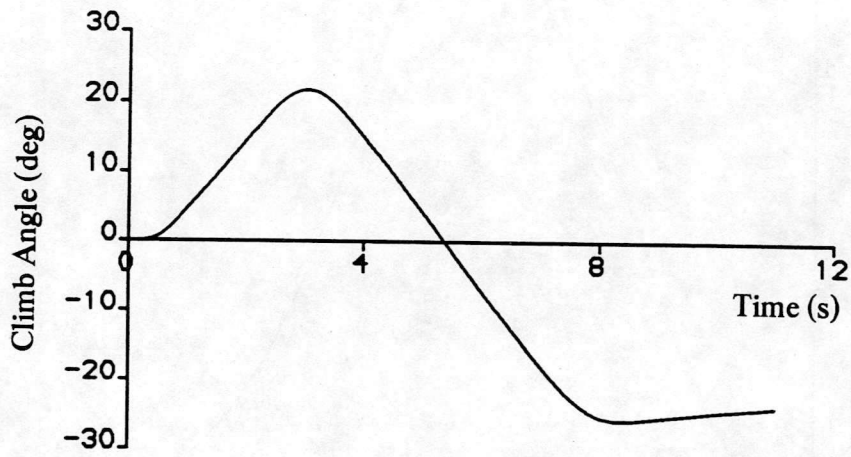


Figure 12 : Climb Angle Distribution in Pull-up/Push-over Manoeuvre

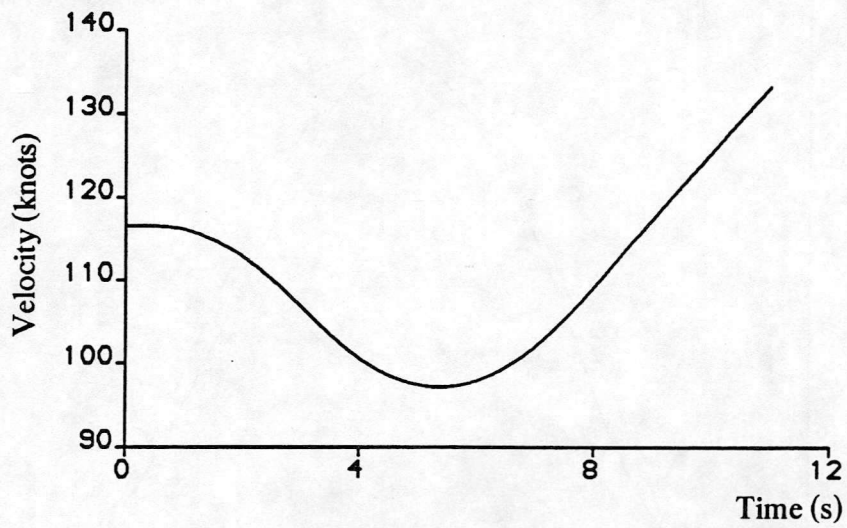
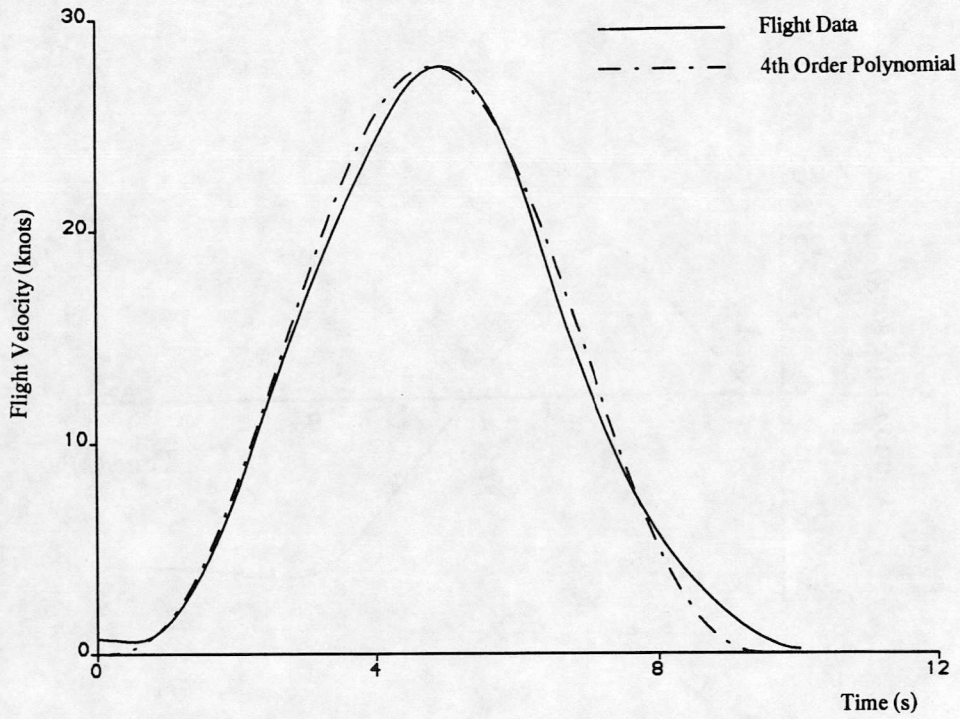
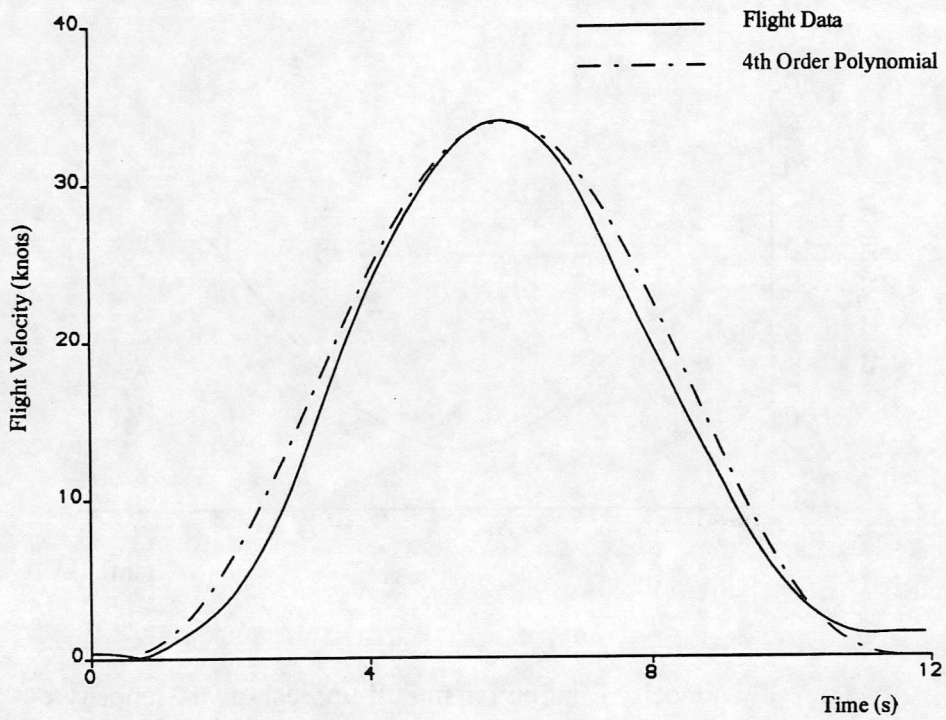


Figure 13 : Velocity Distribution in Pull-up/Push-over Manoeuvre



a) 200ft Side-step



b) 300ft Quick-hop

Figure 14 : Comparison of Velocity from Flight Data and 4th Order Polynomial

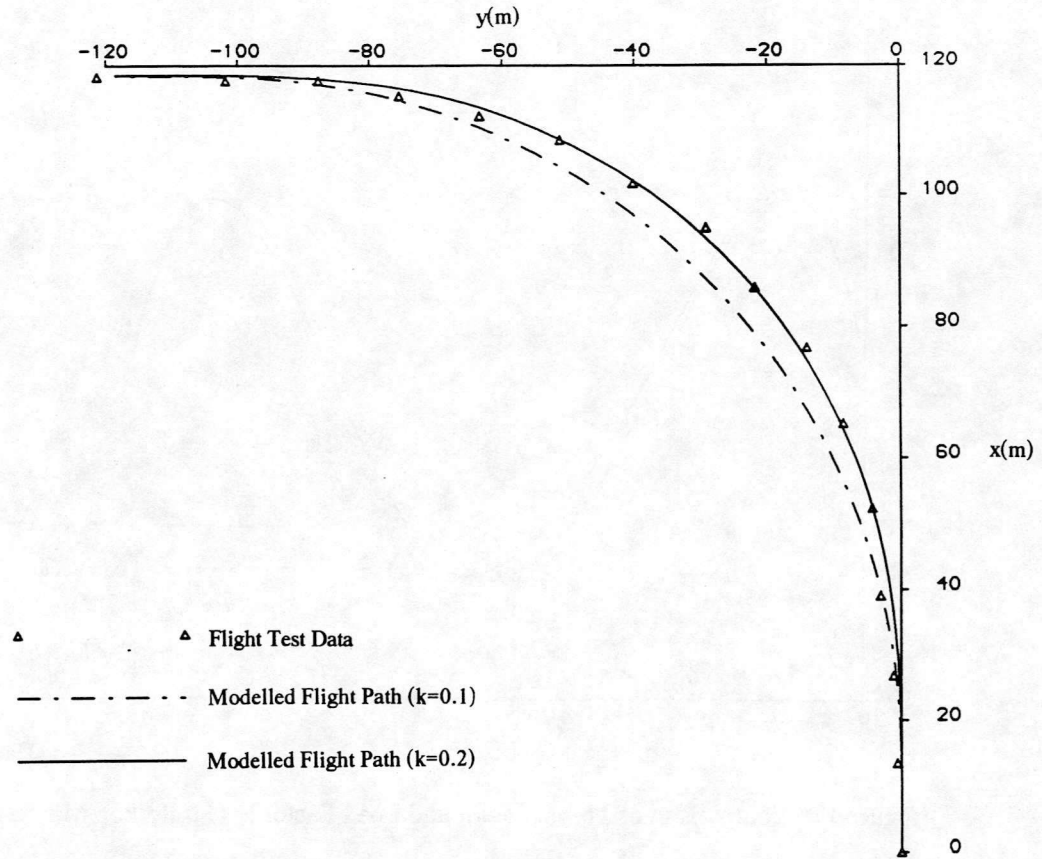


Figure 15 : Comparison of Track from Flight Data and Modelled Flight Path

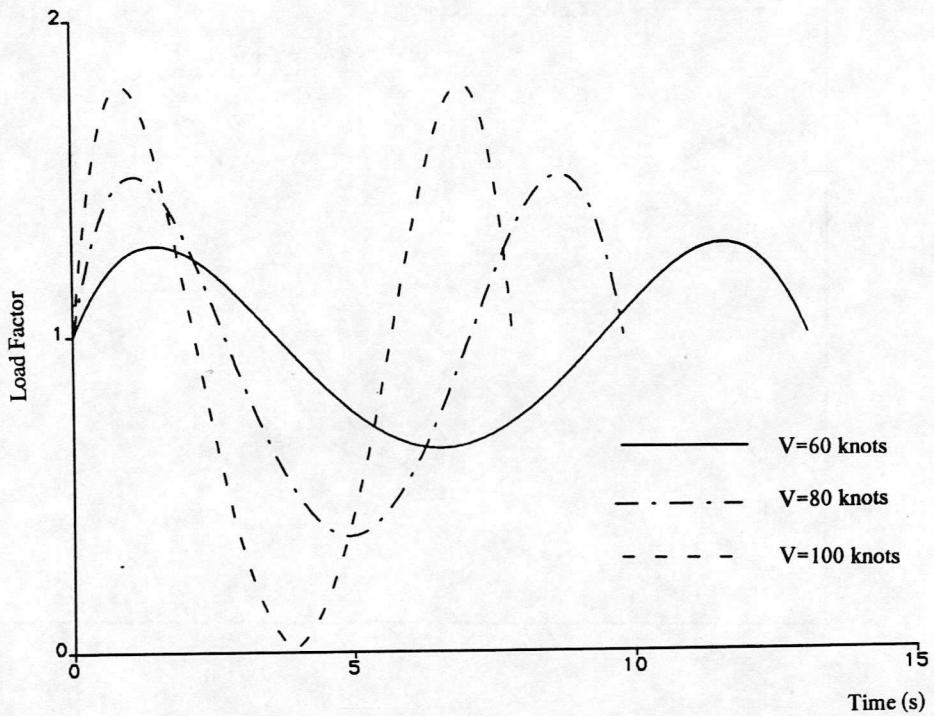


Figure 16 : Flight Path Load Factor Variation in a Hurdle-hop Manoeuvre ($s=400m$, $h=25m$)

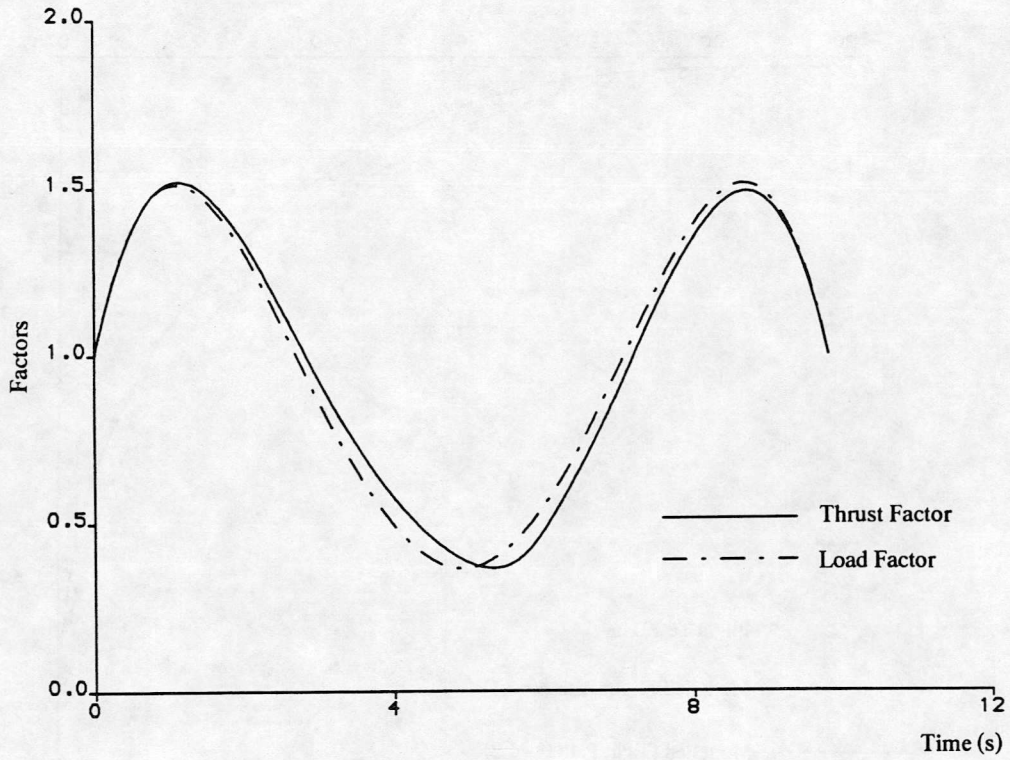


Figure 17 : Comparison of Thrust Factor and Load Factor in Hurdle-hop Manoeuvre
(s=400m, h=25m, V=80 knots)

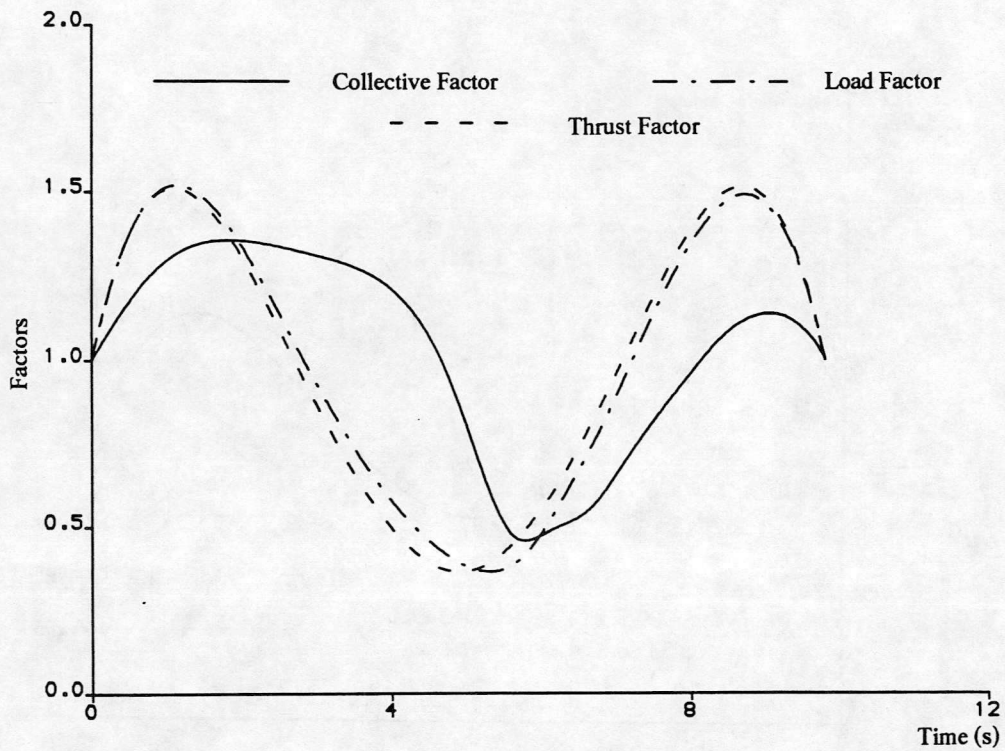


Figure 18 : Comparison of Collective, Thrust, and Load Factors in Hurdle-hop Manoeuvre
(s=400m, h=25m, V=80 knots)

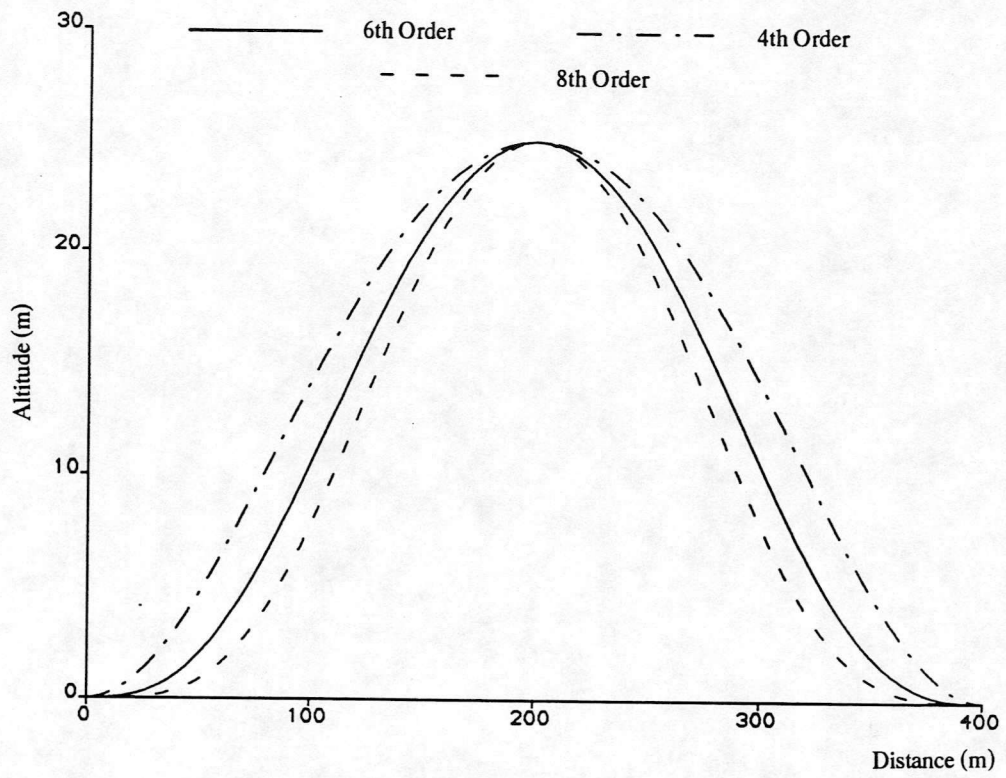


Figure 19 : Effect of Polynomial Order on Hurdle-hop Flight Path Geometry
 (s=400m, h=25m, V=80 knots)

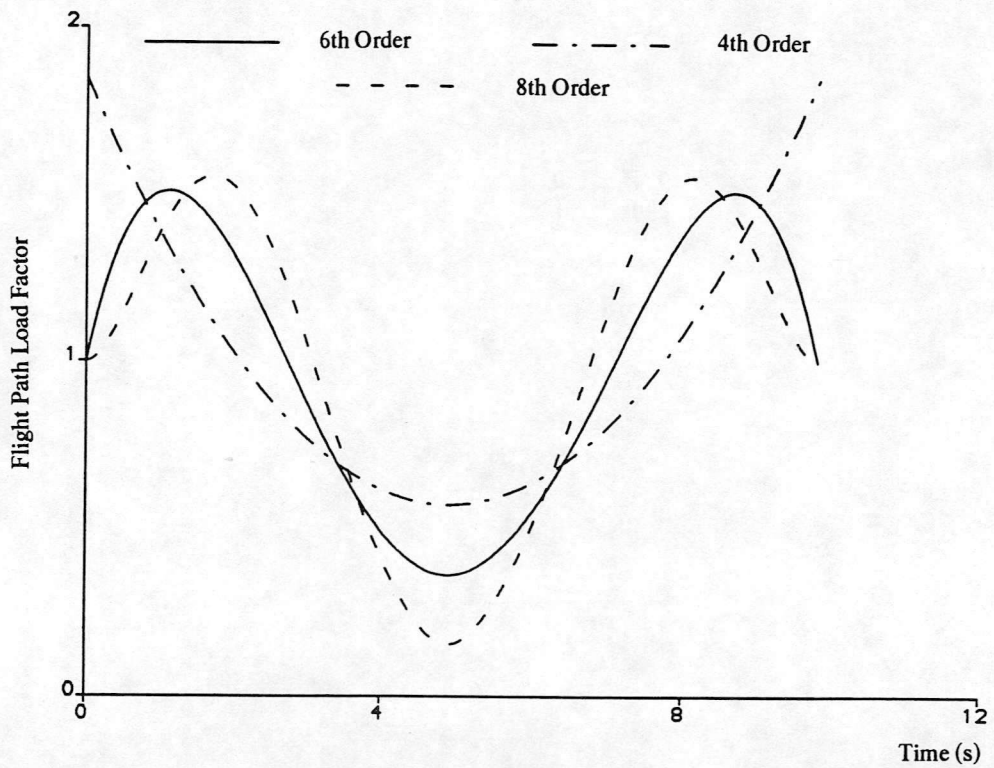
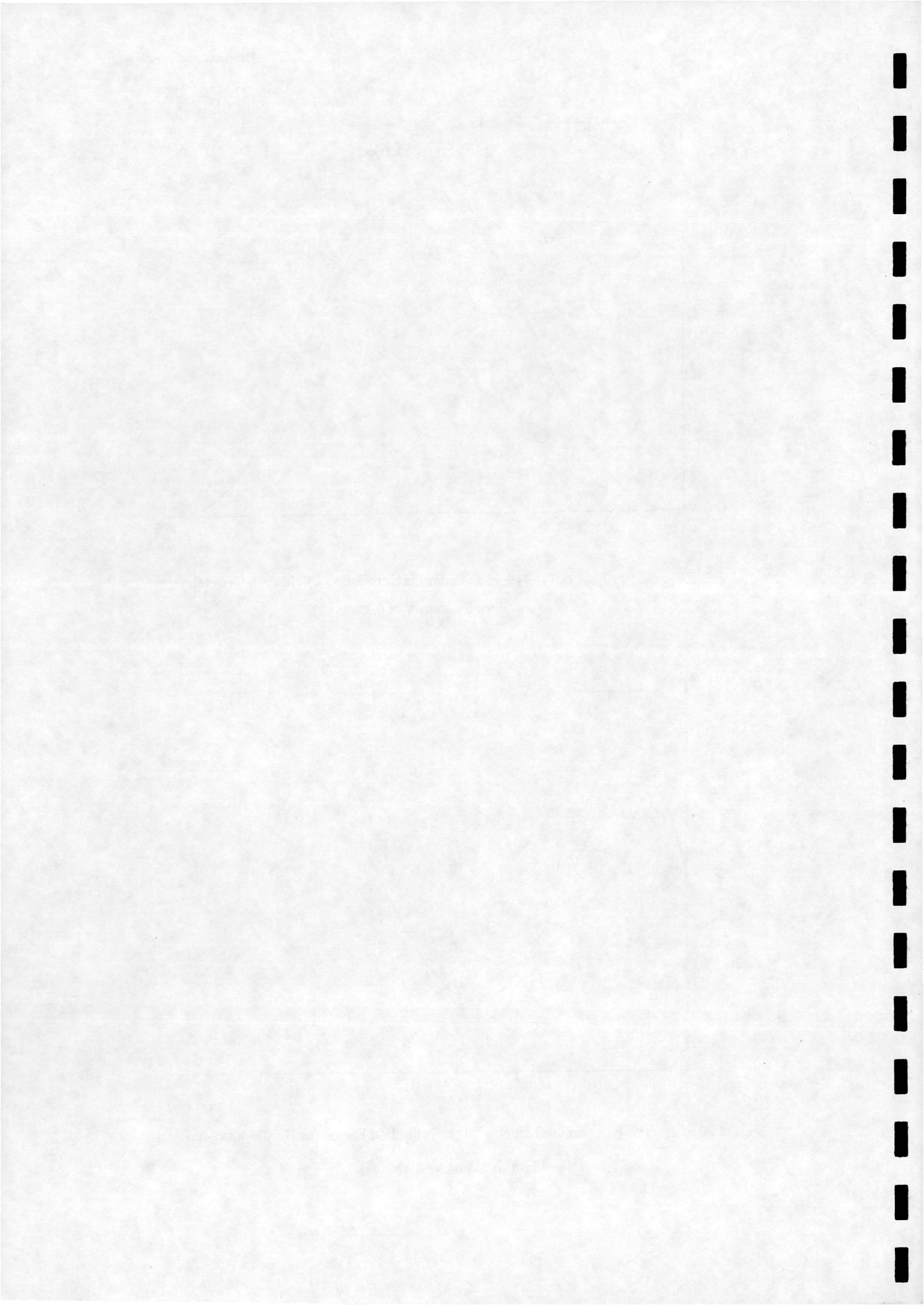


Figure 20 : Effect of Polynomial Order on Flight Path Load Factor for Hurdle-hop Manoeuvre
 (s=400m, h=25m, V=80 knots)





STATIONER
LONDON

